

Stability of Alkoxy-carbonylamidine Prodrugs

Zahra Shahrokh,^{1,3} Eric Lee,¹ Alan G. Olivero,²
Regina A. Matamoros,² Kirk D. Robarge,²
Arthur Lee,² Kenneth J. Weise,²
Brent K. Blackburn,² and Michael F. Powell¹

Received November 3, 1997; accepted December 22, 1997

Purpose. Alkoxy-carbonylamidine prodrug modification was used to mask the positively-charged amidine moiety of an Arg-Gly-Asp peptidomimetic and enhance oral bioavailability. The aqueous stability of ethoxycarbonylamidine (ECA), ethanethiocarbonylamidine (ETCA) and phenoxycarbonylamidine (PCA) prodrugs was examined.

Methods. Degradation was followed by RP-HPLC and rate constants were determined from a degradation scheme defined by product analysis.

Results. ECA gave a pH of maximum stability at pH ~7 and was independent of pH below pH ~4. A novel degradation pathway of ECA, conversion to ethoxycarbonyl-aminocarbonyl, was observed below pH 7. The relative rates below pH 7 were ECA~ETCA<PCA, in the same order of decreasing pK_a of the conjugate acid of the substituted amidino group. Base-catalyzed cleavage of ECA to yield the amidine derivative gave the relative rates ECA<ETCA<PCA, in agreement with the decreasing pK_a of the leaving groups.

Conclusions. The observed rate constants at all pHs were small enough that only 5-30% (depending on the substituent) undesirable degradation is predicted during transit time of the gut. The spontaneous post-absorptive conversion to the amidine drugs at neutral pH is predicted to be 6x greater for the PCA than the ECA prodrugs.

KEY WORDS: peptidomimetic stability; alkoxy-carbonylamidine; ester; prodrug; pH-rate profile; GPII_bIII_a.

INTRODUCTION

Prodrug modification is a unique strategy to rationally modulate the oral bioavailability of drugs (1-4). Prodrugs are designed to alter dissolution/solubility, stability to the gastrointestinal (GI) pH and enzymes, lipophilicity for gut wall epithelial membrane permeability, and enterocyte/liver first pass metabolism (5-10). The challenge in designing prodrugs lies in having adequate in vitro (i.e., shelf life) and in vivo (e.g., pre-absorptive) stability, yet sufficient spontaneous or enzymatic reactivity to generate adequate levels of active compound in the pharmacologically relevant compartment prior to clearance (1-3).

¹ Department of Pharmaceutical R&D, Genentech Inc., 1 DNA Way, South San Francisco, California 94080.

² Department of Bioorganic Chemistry, Genentech Inc., IDNA Way, South San Francisco, California 94080.

³ To whom all correspondence should be addressed. (e-mail: zahra@gene.com)

ABBREVIATIONS: ECA, ethoxycarbonylamidine; ETCA, ethanethiocarbonylamidine; PCA, phenoxycarbonylamidine; ECAC, ethoxycarbonylaminocarbonyl; ETCAC, ethanethiocarbonylaminocarbonyl; PCAC, phenoxycarbonylaminocarbonyl.

This paper describes the chemical stability of amidine prodrugs of a peptidomimetic designed to antagonize the platelet membrane glycoprotein, GPII_bIII_a (11-14). The GPII_bIII_a antagonists are directed at decreasing thrombotic vascular stenosis and myocardial infarction (15-16). The double prodrugs **1**, **9**, and **10** (see structure in Table 1) of the corresponding mono-prodrug, **2**, and the parent drug, **3**, were studied. Despite potent inhibitory activity, **3** showed little oral bioavailability, possibly because of low lipophilicity (see partition coefficient values in Table 1). The double prodrugs were hence synthesized to increase lipophilicity by neutralizing the charged carboxylate and amidino moieties via esterification and alkoxy-carbonyl derivatization, respectively. The prodrugs underwent a novel pathway of acid-catalyzed alkoxy-carbonylamidine conversion to alkoxy-carbonylaminocarbonyl, as well as base-catalyzed cleavage to give the original amidine derivative. The effect of amidine substitution on the relative rates of these degradation pathways, and the implications in prodrug stability and oral bioavailability, are discussed herein.

MATERIALS

Compounds were synthesized at the Bio-organic Chemistry Department, Genentech. Briefly, compounds **1-3** were synthesized by reacting 1 mmol of 4H-1,4-benzodiazepine-4-propanoic acid, 7-[[4-(aminoiminomethyl)-phenyl]ethynyl]-1-methyl-1,2,3,5-tetrahydro-2,5-dioxo-ethyl ester, as previously reported (16) with the corresponding alkoxychloroformate or alkylthiochloroformate in the presence of potassium bicarbonate (5 mmole) in tetrahydrofuran (6 mL) and water (2 mL). Compound **5** (Scheme I) was prepared by subjecting **1** to acid hydrolysis (1 M HCl, ~24 hr at ambient temperature). The products were isolated by solvent extraction and purified by normal phase silica gel chromatography (230-400 mesh, Merck) using ethyl acetate or ethyl acetate/hexane as mobile phase. Compounds were obtained in >95% chemical purity as determined by reverse phase (RP) HPLC, and were characterized by ¹H-NMR, ¹³C-NMR, FAB mass spectrometry and combustion analysis.

Sodium phosphate mono- and di-basic and sodium citrate were from Mallinkrodt, and citric acid from JT Baker, USP grade. HPLC grade acetonitrile (JT Baker), sequential grade trifluoroacetic acid (Pierce), and HPLC grade octanol (Sigma) were used.

METHODS

Buffer Preparation

Low buffer concentrations (>10 mM) were used to minimize buffer catalysis. Phosphate buffer (10 mM) was used at pH 7-9 and 10 mM citrate buffer at pH 2-6. pH values were determined at 5°C, 22°C, and 37°C, and then linearly extrapolated to 60°C. All buffers were aseptically filtered prior to use.

Sample Preparation and Stability Studies

Stability studies were done at a concentration of 5 µg/mL prodrug, approximately 2-4-fold below the solubility limit (Table 1). Fresh 1 mg/mL stock solutions of the double prodrugs **1**, **9**, and **10** in 100% DMSO were diluted to the appropriate

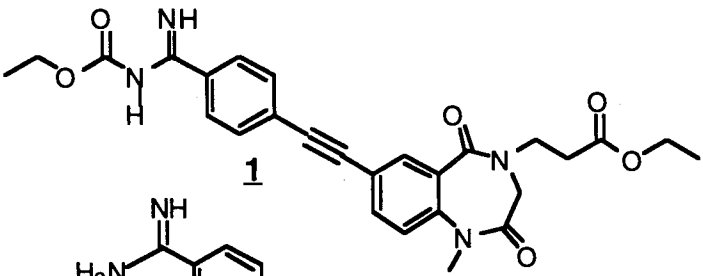
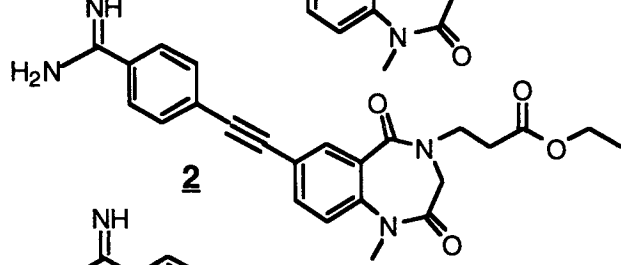
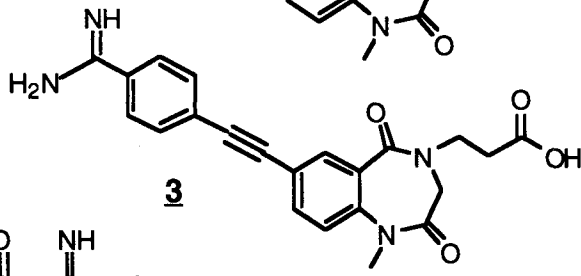
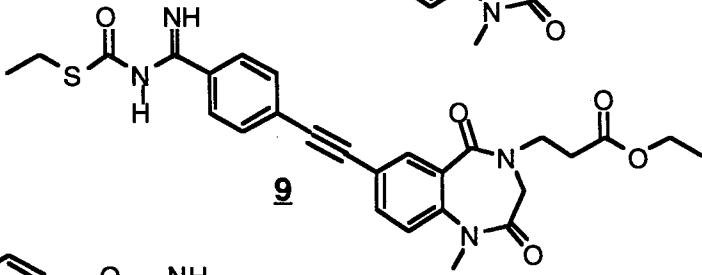
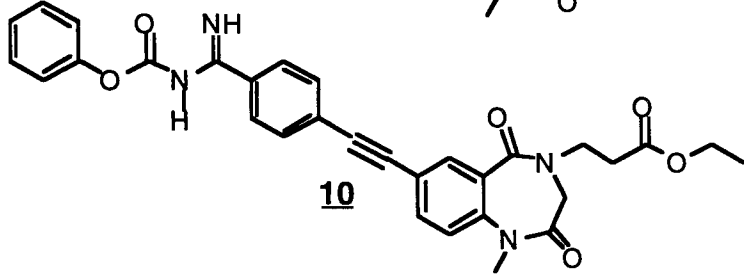
concentration and buffer condition (1% DMSO in final solutions) immediately prior to taking the first time point. Samples (12 mL) and controls were prepared on ice in 15 mL polypropylene Falcon tubes. One mL aliquots (one for each time point) were placed into 1.5 mL HPLC glass vials, crimp-sealed with rubber stoppers, and incubated at various temperatures. One vial was removed at each time point and placed first on ice for 15 sec, then at 4°C (where little degradation was noted) in the refrigerated autosampler of an HPLC for real time analysis. Compound **1** was evaluated at pH 1-9 and 60°C, whereas comparative analysis of degradation kinetics of **1**, **9**, and **10** were made at 37°C and selected pH values only.

Chromatography

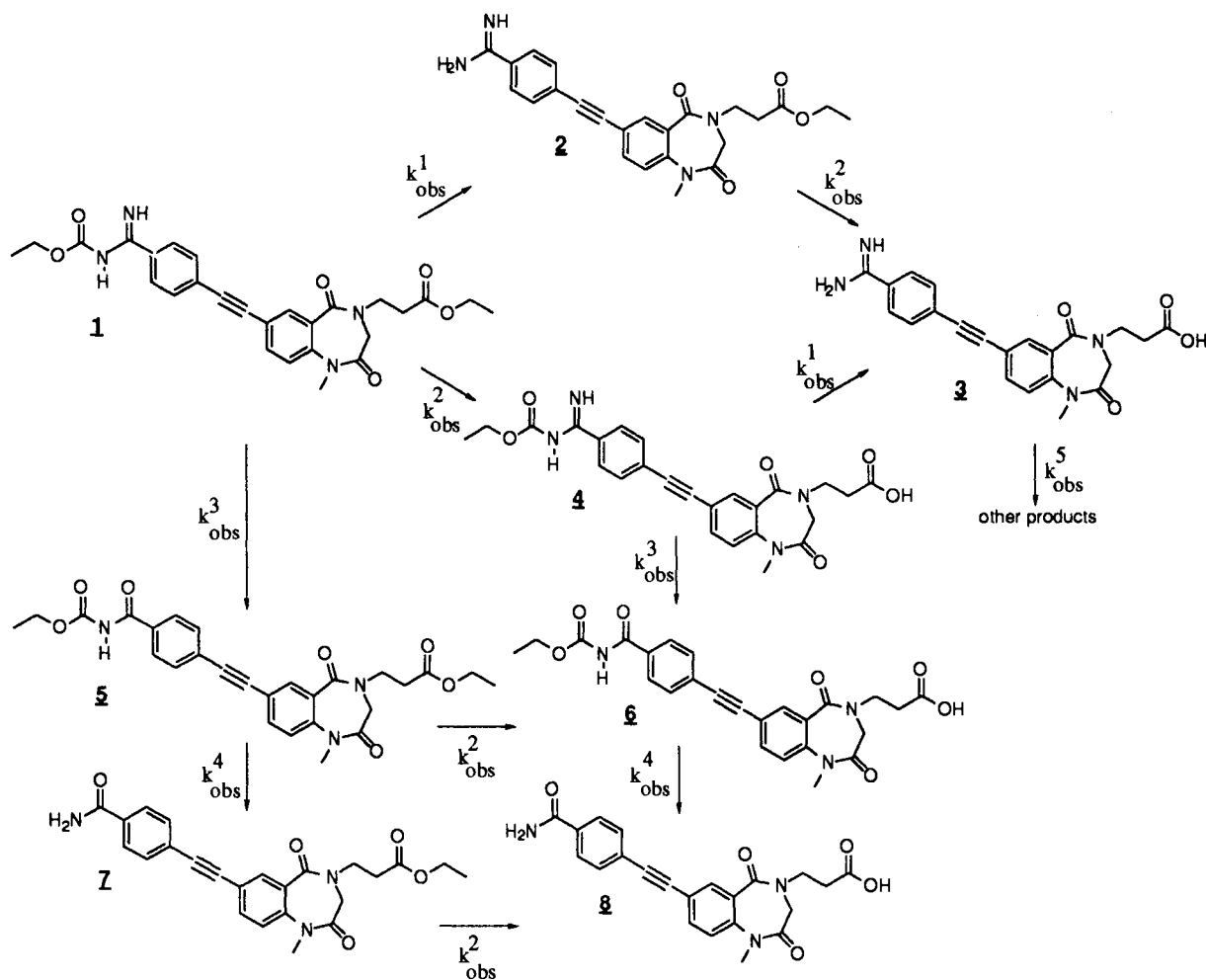
Reversed-phase HPLC (RP-HPLC) was conducted on an HP1090 system equipped with refrigerated autosampler cooled to 4°C for all analyses. A Nucleosil C18 (4.6 x 150 mm) column was used at 40°C, with a 1.5 mL/min flow rate and a linear acetonitrile gradient of 2.5% /min (0.1% TFA in both phases). Compounds eluted in the range of 20 to 45 % acetonitrile. The assay was linear in the range of 100–2000 ng at 214 nm detection; typically 100 μ L (0.5 μ g) was injected.

Mass spectrometry was conducted on fractionated samples ~50-200 pmol) using direct infusion ion spray on a PE SCIEX

Table 1. Structure and Characteristics of the Double (**1**, **9**, **10**) and Mono (**2**) Prodrugs of a GPII_b/III_a Inhibitor, **3**

	Log D	Solubility (mg/mL)
	2.8	0.02
	0.5	.05
	-0.5	>1
	ND	0.005
	ND	0.01

Note: Octanol:buffer partition coefficients at pH 5.0 (Log D), and aqueous solubilities at 22°C and pH ~6 were determined as described in Methods. ND, not determined.



Scheme I. Degradation of an aqueous solution.

API III triple-quadrupole instrument. Molecular masses of the control standards and fractionated samples were calculated using the Hypermass software.

Kinetic Modelling

The mole fraction of each component in the modelling scheme was evaluated from the individual component peak area as a percentage of total peak area. Rate constants were determined using the *iThink*[™] simulation program (High Performance Systems Inc.) and a degradation scheme defined from product analysis (see Scheme I). The kinetic parameters were varied until the simulated reaction curves best fit the experimental data. In some instances the simulated fit using *iThink* program was tested against another compartmental modeling program, SAAM II (SAAM Institute, University of Washington, Seattle) and similar results were obtained ($\pm 3\%$ for the major rate constants).

pK_a Measurements

Determination of pK_a was made by spectrophotometric titration. To adjust pH, a small volume of 0.4 N HCl was added to a 10 mL sample while stirring. A pH probe was directly

inserted into the sample for continuous pH measurements. A 1 mL aliquot was removed and placed in a quartz cuvette for UV spectrophotometry. The aliquot was then returned to the original sample prior to the addition of the next volume of acid. Less than 10% dilution of the sample occurred by this procedure. Spectra (200–500 nm) were collected on a HP 8451A diode array spectrophotometer, corrected for blank buffer (which was independent of pH). The double prodrugs had pronounced peaks at 310 nm and 212 nm at pH 7.1. The extinction coefficients for **1** were 31,940 and 39,080 M⁻¹ cm⁻¹ at these two wavelengths, respectively. Titration of a sample from pH 7.1 down to pH 2 shifted both peaks to longer wavelengths by ~ 10 nm, and decreased the intensity. To calculate pK_a, peak absorbance at 310 nm was fitted to a titration curve according to:

$$\text{Abs}_{310} = [(\text{Abs}_{\text{max}} \times \text{pH})/(\text{pH} + \text{pK}_a)] + \text{Abs}_{\text{min}} \quad (1)$$

where Abs_{max} and Abs_{min} are the limiting absorbances at high and low pHs, respectively.

Solubility Measurements

Aqueous solubility at 22°C was determined by RP-HPLC. A saturated suspension of **1**, **9**, or **10** in water was placed in a bath sonicator for 10 min. Undissolved material was removed

by centrifugation and serially diluted in a 1:1 (vol/vol) mix of acetonitrile and water. These samples were assayed by RP-HPLC, and compared with standards (0.5–2 $\mu\text{g/mL}$) prepared in 50% acetonitrile/water.

Partition Coefficient Determination

Partition coefficient was calculated from the logarithm of the ratio of compound concentrations in octanol and in buffer (10 mM sodium phosphate, pH 5). One mL of a 1–2 mg/mL prodrug dissolved in buffer-saturated octanol was vigorously shaken with 100 mL buffer presaturated with octanol. After phase separation, several dilutions of each phase were made in a 1:1 (vol/vol) mix of acetonitrile and water. The concentration of compound in each phase was determined by RP-HPLC analysis, and compared against a standard curve of 0.5–2 $\mu\text{g/mL}$ samples prepared in 50% acetonitrile.

RESULTS AND DISCUSSION

Degradation Pathways of 1

The degradation of 1 occurred by several pathways, as shown by the number of intermediates observed by RP-HPLC during the time course of the reaction. For example, the time-dependent change in the RP-HPLC profile of 1 studied at pH 8.9 and 60°C is shown in Fig. 1. Several peaks were observed.

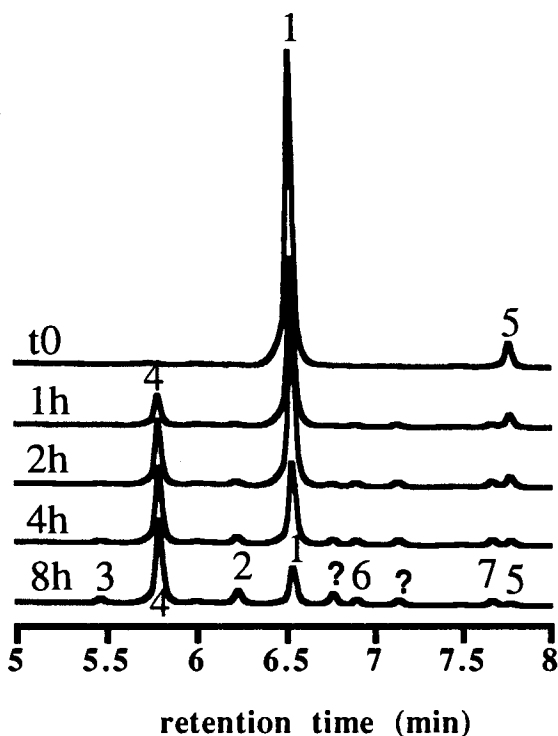


Fig. 1. Time-dependent change in the RP-HPLC chromatographic profile of 1 incubated at pH 8.9 and 60°C. The decrease in 1 was concomitant with an increase in 2, and 4 through 8. Peak 5, which is the ethoxycarbonylamino-carbonyl form (see Scheme I for structures), was present as a ~2% impurity in the original sample, and actually degraded at this high pH. Two other minor peaks were noted and have not yet been characterized.

These were collected, characterized by mass spectrometry, and further identified by coelution with known standards. Minor components (<0.1%) were not identified. The double prodrug 1 degraded by three pathways: ECA hydrolysis to give 2 (rate constant k_{obs}^1), ester hydrolysis to give 4 (k_{obs}^2), and ECA conversion to ethoxycarbonylamino-carbonyl (ECAC) to give 5 (k_{obs}^3) (see Scheme I). Compounds 2, 4, or 5 further degraded to give 3, 6, 7, and 8, respectively (fitting the data suggested that 3 might also degrade at alkaline pH to other products (rate constant k_{obs}^5), although this was a small contributor to the overall degradation scheme.

To determine the observed rate constants (k_{obs}^i) for a given pathway, *i*, at each reaction pH the kinetic data of 1–6 were fitted simultaneously. The computation of eight independent rate constants is complex because of the large number of variables, and because small amounts of products were already present at t_0 . Fortunately, the reaction scheme can be simplified by assuming that certain rate constants are equivalent. For example, the rate of ester hydrolysis is likely to be independent of the derivatization of the amidine terminus; hence, the same rate constant (k_{obs}^2) has been used for conversion of 1 to 4, 2 to 3, and 5 to 6. Likewise, the rate of ECA conversion to ECAC is expected to be independent of the derivatization at the carboxy terminus; i.e., k_{obs}^3 for conversion of 1 to 5 is the same as that for 4 to 6.

Rate Law for ECA Cleavage to Yield the Amidine Derivative (k_{obs}^1)

Whereas hydrolytic ECA cleavage of 1 leading to 2 was minimal and pH-independent below pH 7, specific base-catalyzed cleavage was observed at high pH (Fig. 2A). The empirical rate law for k_{obs}^1 is thus:

$$k_{\text{obs}}^1 = k_0^1 + k_{\text{HO}^-}^1 [\text{HO}^-] \quad (2)$$

where $k_{\text{HO}^-}^1$ and k_0^1 are the apparent hydroxide and water catalyzed rate constants for k_{obs}^1 , respectively. A least squares fit of the data to equation (2) gave $k_{\text{HO}^-}^1 = 4.7 \pm 2.8 \text{ M}^{-1} \text{ min}^{-1}$, and $k_0^1 = 0.36 \pm 0.09 \times 10^{-4} \text{ min}^{-1}$. This pathway was a minor one and accounted for less than 1% of total degradation of ECA, even at alkaline pH.

The mechanisms for ECA and PCA cleavage are probably similar to those described previously for carbamate derivatives of simple amines, one, involving hydroxide ion attack at the carbonyl carbon for the alkylcarbamates, and the other, hydroxide attack on the deprotonated amidine for the phenylcarbamates (17–21). A broad water term at pH –1 to 7 has been reported for carbamoylated alkylamines (18,20,21), as has specific base-catalyzed cleavage (20,21).

Rate-Law for Ester Hydrolysis (k_{obs}^2)

The pH-rate profile for ester hydrolysis showed a classical U-shaped pH-dependence (22–24) with predominant acid-catalyzed hydrolysis below pH 3, a broad spontaneous reaction in the pH range of 3 to 7, and specific base-catalysis above pH 7. Data were fitted to the semi-empirical equation:

$$k_{\text{obs}}^2 = k_{\text{H}^+}^2 [\text{H}^+] + k_0^2 + k_{\text{HO}^-}^2 [\text{HO}^-] \quad (3)$$

The apparent rate constants $k_{\text{H}^+}^2$, k_0^2 , and $k_{\text{HO}^-}^2$ denote catalysis by hydronium ion, water, and hydroxide ion, respectively. Non-

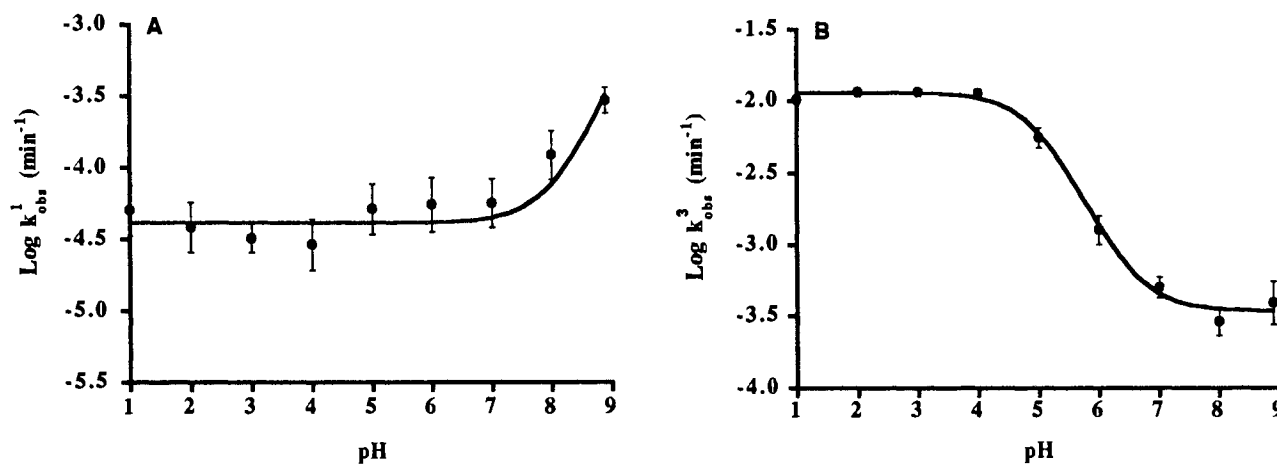


Fig. 2. (A) Effect of pH on the observed rate of ECA cleavage to the amidine derivative, k_{obs}^1 at 60°C (see text for details). A hydroxide catalyzed reaction is seen above pH ~7. The solid line is the non-linear least square fit to the data according to equation (2). (B) Effect of pH on the observed rate of ECA conversion to ECAC, k_{obs}^3 , at 60°C (see text for details). Protonation of the amidino group gives ~2-orders of magnitude faster reaction than that by the neutral form. A titration curve fitted to the data to equation (5) gives a pK_a of ~5.

linear least squares analysis gave $k_{\text{H}^+}^2 = 390 \pm 140 \times 10^{-4} \text{ M}^{-1} \text{ min}^{-1}$, $k_0^2 = 0.39 \pm 0.13 \times 10^{-4} \text{ min}^{-1}$, and $k_{\text{H}_2\text{O}}^2 = 13.1 \pm 4.2 \text{ M}^{-1} \text{ min}^{-1}$. The significant variation in k_{obs} between pH 3 and 7 was because ester hydrolysis constituted <0.1% of the overall reaction.

Rate Law for Conversion of ECA to ECAC (k_{obs}^3)

This novel reaction was the major degradation pathway for **1** at low pH. The pH-rate profile was sigmoidal, showing a plateau below pH 4 and a minimum near pH 7 (Fig. 2B). As shown in Scheme II, this profile may be due to the different rates of water catalysis of the unprotonated (k_0^3) and the protonated amidino species (k_0^3). Water attack on the amidino carbon, giving a tetrahedral intermediate, is predicted to be more reactive for the protonated than the neutral form. Further water attack, rearrangement, and release of ammonia leads to the formation of the alkoxy-carbonylaminocarbonyl product.

Based on this mechanism the rate law for k_{obs}^3 is:

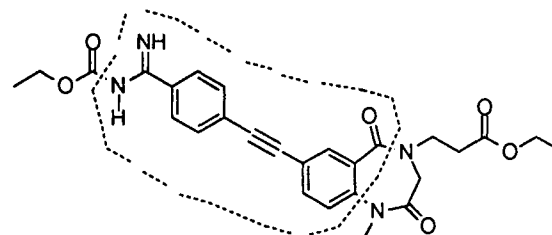
$$k_{\text{obs}}^3 = f k_0^3 + f' k_0^3 \quad (4)$$

where f and f' are the fractions of the unprotonated and the protonated species, respectively. The expression for f can be rearranged to give:

$$f = \frac{1}{1 + 10^{(\text{pK}_a - \text{pH})}} \quad (5)$$

A least squares fit to the data gave $k_0^3 = 3.9 \pm 0.5 \times 10^{-4} \text{ min}^{-1}$ and $k_0^3 = 114 \pm 4 \times 10^{-4} \text{ min}^{-1}$, and a pK_a value of 5.0 ± 0.1 at 60°C. The low pK_a is not surprising in that the amidino group is conjugated to a large segment of the molecule (drawn in dotted lines in Scheme II).

Spectrophotometric determination of the pK_a of **1** was made by UV spectroscopy. Fitting of the data to the titration equation (1) gave a pK_a value of 5.58 ± 0.06 at 22°C. Considering that the pK_a of amines increases with a decrease in temperature, the spectrophotometrically determined pK_a at 22°C was consistent with the kinetically determined pK_a at 60°C.



Scheme II.

Total Degradation Profiles

The pH-dependence of the total observed degradation rate constant for **1** ($k_{\text{obs}}^{\text{tot}}$) at 60°C is shown in Fig. 3. The profile has a minimum at pH 7 and is pH-independent below pH ~4. At any pH, $k_{\text{obs}}^{\text{tot}}$ is the sum of the rate constants k_{obs}^1 , k_{obs}^2 , and k_{obs}^3 , at that pH. Summing equations (2), (3), and (4) that describe the pH-dependence of these individual rate constants shows

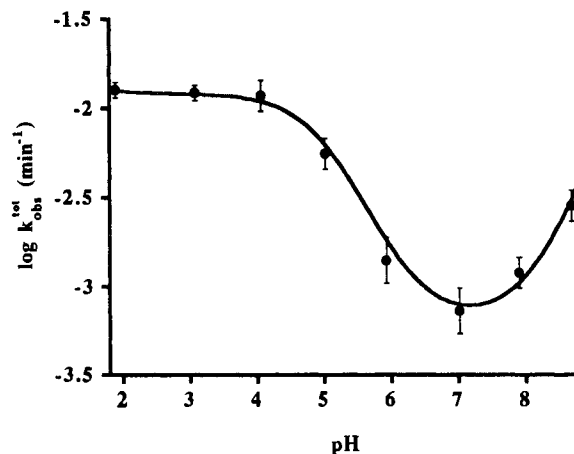


Fig. 3. Effect of pH (at 60°C) on the overall stability of **1**. The solid line is the data fitted to expression (6) in the text.

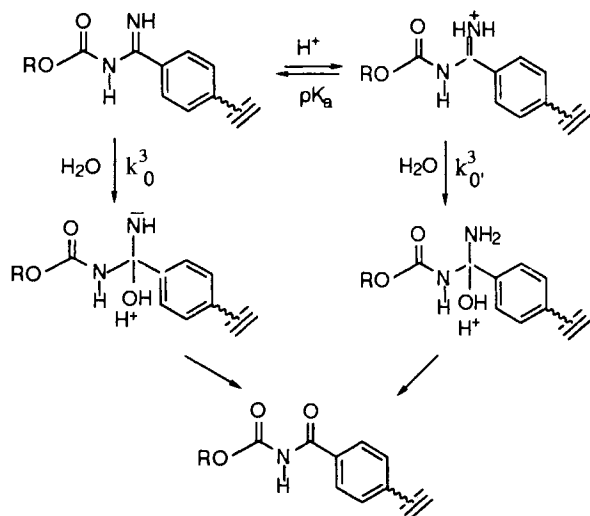
that the pH-dependence of $k_{\text{obs}}^{\text{tot}}$ is made of contributions from acid- and base-catalyzed reactions ($k_{\text{H}^+}^{\text{tot}}$ and $k_{\text{HO}^-}^{\text{tot}}$, respectively), as well as from water catalysis of the protonated (k_0^{tot}) and the unprotonated (k_0^{tot}) amidino forms:

$$\log k_{\text{obs}}^{\text{tot}} = \log \left[k_{\text{H}^+}^{\text{tot}} \times 10^{-\text{pH}} + \frac{k_0^{\text{tot}}}{1 + 10^{(\text{pK}_a - \text{pH})}} \frac{k_0^{\text{tot}}}{1 + 10^{(\text{pH} - \text{pK}_a)}} \right. \\ \left. + k_{\text{HO}^-}^{\text{tot}} \times 10^{-(\text{K}_w - \text{pH})} \right] \quad (6)$$

A least squares fit to the data in Figure 3 using equation (6), a pK_a of 5.0 and pK_w of 13.017 gave $k_{\text{H}^+}^{\text{tot}} = 338 \pm 180 \times 10^{-4} \text{ min}^{-1}$, $k_{\text{H}^+}^{\text{tot}} = 52 \pm 14 \text{ M}^{-1} \text{ min}^{-1}$, $k_0^{\text{tot}} = 6.2 \pm 1.8 \times 10^{-4} \text{ min}^{-1}$, $k_0^{\text{tot}} = 121 \pm 8 \times 10^{-4} \text{ min}^{-1}$.

Effect of Temperature on the Stability of 1

The temperature dependence of $k_{\text{obs}}^{\text{tot}}$ was evaluated at pH 2 and 6 in the temperature range of 5 to 60 °C. The thermodynamic parameters were obtained from an Eyring plot defined by $\ln k_{\text{obs}}/T = \ln(k/h) + \Delta S^\ddagger - \Delta H^\ddagger/RT$, where k is Boltzmann constant, h is Planck's constant, R is Universal gas constant, and ΔH^\ddagger and ΔS^\ddagger are the transition state enthalpy and entropy, respectively. From the slopes and intercepts of these plots, ΔH^\ddagger and ΔS^\ddagger values of $21.3 \pm 0.6 \text{ kcal}\cdot\text{mol}^{-1}$ and $-2 \pm 1.8 \text{ cal}\cdot\text{mol}^{-1}\cdot\text{K}^{-1}$ at pH 2, and $18.3 \pm 2.3 \text{ kcal}\cdot\text{mol}^{-1}$ and $-13.4 \pm 7.3 \text{ cal}\cdot\text{mol}^{-1}\cdot\text{K}^{-1}$ at pH 6 were calculated. Since ECA conversion to ECAC was the major governing reaction below pH 7, these thermodynamic parameters were similar at pH 2 and pH 6, and also were similar to those reported previously for hydrolysis reactions (23). A negative ΔS^\ddagger observed from these data is suggestive of a bi-molecular reaction (25), and is consistent with direct involvement of water in the conversion of the ECA to ECAC, as shown in Scheme III.



Scheme III. Mechanism of alkoxy-carbonylamidine conversion to alkoxy-carbonylaminocarbonyl derivative.

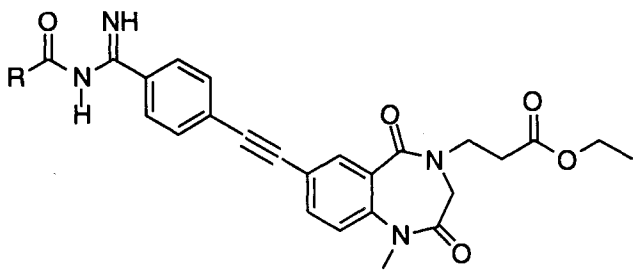
Amidine Prodrug Substituent Effect on Relative Stability of the Prodrugs



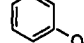
The amidine prodrug substituent effect on the susceptibility to hydrolytic processes was investigated for the ethanethio-

carbonylamidine (ETCA, **9**) and phenoxy-carbonylamidine (PCA, **10**) derivatives. Compounds **9** and **10** showed similar degradation products as those described for **1** in Scheme I, but markedly different hydrolysis rates. Table 2 shows the relative rate constants at 37°C and pH 2, 6, and 9. At pH 6 where ECA conversion to the amidine derivative was minimal for **1**, the rate constant k_{obs}^1 was ~15x and ~60x greater for **9** and **10**, respectively; at pH 9, k_{obs}^1 was ~25x and ~95x greater. The faster rates of PCA > ETCA > ECA is consistent with the better leaving group ability, as reflected in the decreasing leaving group pK_a (16, 10.5, 9.9 for ethanol, thioethanol, and phenol, respectively (26)). On the other hand, the rate of conversion of ECA to ECAC derivative (k_{obs}^3) was comparable for **1** and **9**, but 4x faster for **10** at pH 2 and 9. This may be due to the electron withdrawing phenoxy-carbonyl substituent (with its extended conjugation) and the lower pK_a of the conjugate acid of the amidino moiety, giving the carbonyl carbon a greater δ^+ charge and making it more susceptible to water attack. Indeed the spectrophotometrically determined pK_a for the protonated amidino group of **10** was 3.6, ~2 units lower than for **1**. Examination of the over-all pH-rate profile of **10** (Fig. 4) indicated that the degradation rates were at least an order of magnitude greater than for **1** at all pHs, and that the pH of maximum stability was shifted to ~0.5 unit lower value compared to **1**. Expectedly, k_{obs}^2 values were similar for the three compounds which had the same ethyl ester moiety at their carboxylic terminus. This observation further confirms an assumption made in the kinetics analysis of scheme I, that there is little influence of the amidine derivatization on ester hydrolysis rate.

Stability Under Physiological Conditions

To predict the physiological stability of **1**, the rate constants at 37°C were calculated from the Arrhenius parameters, and the appropriate autoprotolysis constants (which is expected to shift the pH profile to lower values by ~0.5 pH unit in going from 60°C to 37°C). Using the GI tract transit parameters (~1.5 hr in stomach at pH 2-4, ~4 hr in small intestine ranging in pH from 5-7), only ~5% spontaneous degradation of **1** was predicted. Similar examination of the stability of **10** using the pH-dependence of total degradation at 37°C (Fig. 4), predicted ~30% degradation due only to pH during the GI transit time, ~6x greater than for **1**. On the other hand, spontaneous conversion of **10** to the amidine/ester monoprodrug under the conditions relevant to the pharmacological compartment of blood (pH 7, 37°C, 4 hrs) was estimated at ~20%, compared to ~0.5% for **1**; this would predict that the contribution of spontaneous conversion to the oral bioavailability is 40x greater for **10** than for **1**, since the ester mono-prodrug thus generated should convert rapidly to the active compound by plasma esterases (27,28). In addition to spontaneous hydrolysis, however, conversions by enzymes in the GI tract (29,30) and in plasma (9,31-33) are expected to modulate the in vivo stability of these prodrugs. For example, **10** completely degraded within ~1 min in a gavage fluid of rabbit jejunum, compared to **1** which had a half life of ~20 min at 37°C. Also, IV administration to rats showed nearly complete bioconversion of **10**, compared to only ~5% for **1**, consistent with their in vitro plasma stability (90% and 5% conversion of **10** and **1**, respectively, within 30 minutes in rat plasma) (34). The ultimate oral bioavailability is a balance

Table 2. Degradation Rate Constants (at 40°C) for Substituents at the Amidine Moiety of **2**


compound	R	$k_{\text{obs}}^1 (\text{min}^{-1}) \times 10^4$			$k_{\text{obs}}^2 (\text{min}^{-1}) \times 10^4$		
		pH 2	pH 6	pH 9	pH 2	pH 6	pH 9
1		0.03±0.02	0.08±0.03	0.32±0.02	9.3±2.7	2.2±0.2	0.13±0.03
9		1.0±0.3	1.3±0.3	7.7±0.3	5.2±1.0	1.0±0.5	0.05±0.04
10		3.3±1.0	5.3±0.7	27.5±1.2	41.7±8.3	1.3±1.2	0.50±0.17

Note: Each compound was incubated at 5 $\mu\text{g/mL}$ in 0.1 M HCl (pH 2), 10 mM sodium citrate (pH 6), and 10 mM sodium phosphate (pH 9). The kinetics of degradation was followed by RP-HPLC as described in Methods. Alkoxycarbonylamidino cleavage rate constant, k_{obs}^1 , increased in the order $1 < 9 \ll 10$, whereas the rate constant for alkoxycarbonylamidino conversion to alkoxycarbonylaminocarbonyl, k_{obs}^2 , was $1 \cong 9 \ll 10$. The ester hydrolysis rate constant, k_{obs}^3 , was predictably the same for all compounds. The fits to the data for **9** and **10** were poorer than for **1**, in part due to the presence of additional unidentified degradation components, and in part due to the adsorption/low solubility of the compounds. The extremely low solubility of **9** gave variable loss in total recovery; data from time points with >80% total recovery were used.

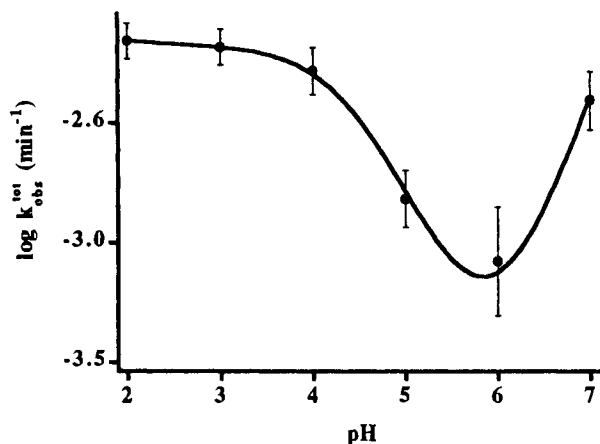


Fig. 4. Effect of pH (at 37°C) on the overall stability of **10**. The fitted curve uses expression (6) in the text. The pK_a calculated from this profile was 4.2 (at 37°C), consistent with that obtained spectrophotometrically (at 22°C).

of the undesirable processes (e.g., pre-absorptive degradation, first pass metabolism, organ clearance) and the desirable permeability and post-absorptive conversion processes. Despite complete bioconversion of **10**, the oral bioavailability was low (~5%) and the same as for **1** (4), at least in part because of the greater lability to pre-systemic enzymatic degradation.

In summary, care should be taken for the synthesis and storage of the alkoxycarbonylamidino prodrugs by minimizing contact with acid and with water. The reaction rates at pH 2-6 and 37°C are slow enough that <30% degradation should occur due to pH alone. Finally, the rank order of chemical degradation and enzymatic conversion is the same for these prodrugs; it appears that for improved oral bioavailability a prodrug with greater bioconversion potential than **1**, but less

degradation potential than **10** is needed (this is the subject of a forthcoming manuscript by Olivero et al., in preparation).

ACKNOWLEDGMENTS

We thank the following Genentech colleagues: Katrina Brabham and Beatrice Costales for assistance with pK_a determinations, Beth Gillece-Castro for mass spectrometry, and Bob Strickley for discussions of the kinetics and valuable comments on the manuscript.

REFERENCES

- H. Buundgaard. The double prodrug concept and its applications. *Adv. Drug Delivery Rev.* **3**:39-65 (1989).
- N. Bodor and J. J. Kaminski. Prodrugs and site-specific chemical delivery systems. In: Allen, ed. *Annual Reports in Medicinal Chemistry*, Academic Press, New York, 1987, Vol. 22, pp. 303-313.
- D. Shan, M. G. Nicolaou, R. T. Borchardt, and B. Wang. Prodrug strategies based on intramolecular cyclization reactions. *J. Pharm. Sci.* **86**:765-7 (1997).
- R. J. Jones and N. Bischoberger. Minireview: nucleotide prodrugs. *Antiviral Res.* **27**:1-17 (1995).
- S. H. Yalkowsky, A. A. Sinkula, and S. C. Valvani. *Physical Chemical Properties of Drugs*. Marcel Dekker Inc., New York, 1980.
- J. B. Dressman, P. Bass, W. A. Ritschel, D. R. Friend, A. Rubinstein, and E. Ziv. Gastrointestinal parameters that influence oral medications. *J. Pharm. Sci.* **82**:857-872 (1993).
- J. Blanchard. Gastrointestinal absorption. II. Formulation factors affecting drug bioavailability. *Amer. J. Pharm. Sci. Suppl. Publ. Health* **150**:132-151 (1978).
- G. M. Pauletti, S. Gangwar, G. T. Knipp, M. M. Nerurkar, F. W. Okumu, K. Tamura, T. J. Sahaan, and R. T. Borchardt. Structural requirements for intestinal absorption of peptide drugs. *J. Controlled Release* **41**:3-17 (1996).
- J. Alexander, D. S. Bindra, D. Glass, M. A. Holahan, M. L. Renyer, G. S. Rork, G. R. Sitko, M. T. Stranieri, R. F. Stupimdkki, and H. Veerapanane. Investigation of (Oxodioxenyl)methyl carbamates as nonchiral bioreversible prodrug moieties for chiral

- amines. *J. Med. Chem.* **39**:480–6 (1996).
10. B. A. Boucher. Fosphenytoin: A novel phenytoin prodrug. *Pharmacotherapy* **16**:771–91 (1996).
 11. E. Rouslahti and M. D. Pierschbacher. New perspectives in cell adhesion: RGD and integrins. *Science* **238**:491–497 (1987).
 12. T. Yasuda, H. K. Gold, C. Kohmura, et al. Intravenous and endobronchial administration of G4120, a cyclic Arg-Gly-Asp-containing platelet GPIIb/IIIa receptor-blocking pentapeptide, enhances and sustains coronary arterial thrombolysis with rt-PA in a canine preparation. *Arterioscl. Thromb.* **13**:738–747 (1993).
 13. B. K. Blackburn and T. R. Gadek. Glycoprotein IIb/IIIa antagonists. *Annual Reports in Medicinal Chemistry*. **28**:79–88 (1993).
 14. R. S. McDowell, B. K. Blackburn, T. R. Gadek, et al. From peptide to non-peptide. 2. The de Novo design of potent, non-peptidic inhibitors of platelet aggregation based on a benzodiazepinedione scaffold. *J. Am. Chem. Soc.* **116**:5077–5083 (1994).
 15. The EPIC Investigators. Use of a monoclonal antibody directed against the platelet glycoprotein IIb/IIIa in high-risk coronary angioplasty. *New Engl. J. Med.* **330**:956–1007 (1994).
 16. T. Weller, L. Alig, M. Beresini M, et al. Orally active fibrinogen receptor antagonists. 2. Amidoximes as prodrugs of amidines. *J. Med. Chem.* **39**:3139–3147 (1996).
 17. L. W. Dierker and T. Higuchi. Rates of hydrolysis of carbamate and carbonate esters in alkaline solution. *J. Pharm. Sci.* **52**:852–857 (1963).
 18. A. F. Hegarty and L. N. Frost. Elimination-addition mechanism for the hydrolysis of carbamates. Trapping of an isocyanate intermediate by an *o*-amino-group. *J. Chem. Soc. Perkin Trans II*: 1719–1728 (1973).
 19. A. F. Hegarty, L. N. Frost, J. H. Coy. The question of amide group participation in carbamate hydrolysis. *J. Org. Chem.* **39**:1089–1093 (1974).
 20. T. Vontor, J. Socha, and M. Vecera. Kinetics and mechanism of hydrolysis of 1-Naphthyl N- Methyl- and N,N-Dimethylcarbamates. Collection Czechoslov. *Chem. Commun.* **37**:2183–2196 (1972).
 21. T. Vontor and M. Vecera. Kinetics and mechanism of hydrolysis of substituted phenyl carbamates. Collection Czechoslov. *Chem. Commun.* **38**:516–522 (1973).
 22. G. M. Loudon. Mechanistic interpretation of pH-rate profiles. *J. Chem. Educ.* **68**:973–84 (1991).
 23. M. F. Powell, A. Becker, A. Magill. Nonsteroidal anti-psoriatic prodrugs: Hydrolysis and aminolysis of naphthyl esters in aqueous solution. *Int. J. Pharmaceutics* **35**:61–71 (1987).
 24. H. Bundgaard, E. Falch, C. Larsen, G. L. Mosher, and T. J. Mikkelsen. Pilocarpine prodrugs. II. Synthesis, stability, bioconversion, and physicochemical properties of sequentially labile pilocarpine acid diesters. *J. Pharm. Sci.* **75**:775–783 (1986).
 25. C. Bamford and C. Typer. *Chemical Kinetics*. Elsevier, New York, 1977, p.16.
 26. S. Budavari, M. J. O'Neil, A. Smith, P. E. Heckelman, and J. F. Kinnery. *The Merck Index*. Whitehouse Station, NJ: Merck & Co., Inc., 1996.
 27. B. LaDu. Plasma esterase activity and the metabolism of drugs with ester groups. *Ann. N. Y. Acad. Sci.* **179**:684–694 (1993).
 28. F. W. Williams. Clinical significance of esterases in man. *Clin. Pharmacokin.* **10**:392–403 (1985).
 29. J. C. Pekas. Intestinal hydrolysis, metabolism and transport of a pesticidal carbamate in pH 6.5 medium. *Toxicol. Appl. Pharmacol.* **23**:62–70 (1972).
 30. M. Inoue, M. Morikawa, M. Tsuboi, and M. Sugiura. Species difference and characterization of intestinal esterase on the hydrolyzing activity of ester-type drugs. *Japan J. Pharmacol.* **29**:9–16 (1979).
 31. L. W. Brown and A. A. Forist. In vitro and in vivo hydrolysis of 4-benzoylphenyl N- methylcarbamate. *J. Pharm. Sci.* **62**:145–146 (1973).
 32. K. T. Hansen, P. Faarup, and H. Bundgaard. Carbamate ester prodrugs of dopaminergic compounds: Synthesis, stability, and bioconversion. *J. Pharm. Sci.* **80**:793–798 (1991).
 33. J. Alexander, R. A. Fromtling, J. A. Bland, B. A. Pelak, and E. C. Gilfillan. (Acyloxy)alkyl carbamate prodrugs of norfloxacin. *J. Med. Chem.* **34**:78–81 (1991).
 34. A. G. Olivero, B. K. Blackburn, K. D. Roburge, R. A. Matamoros, A. Lee, K. Weese, J. P. Burnier, S. Bunting, K. C. Refino, D. Wu, M. T. Lipari, C. Pater, G. G. Deguzman, T. F. Zioncheck, T. Weller, and B. Stainer. Design, synthesis and evaluation of oral GP IIB/IIIa antagonists: A prodrug approach. 212th Am. Chem. Soc. Annual Meeting Abstracts 130a, 1996.